


TUMOR MARKERS AND SIGNATURES

Time-dependent changes in proliferation, DNA damage and clock gene expression in hepatocellular carcinoma and healthy liver of a transgenic mouse model

Soha A. Hassan^{1,2} | Christian Schmithals³ | Maike von Harten³ | Albrecht Piiper³ | Horst-Werner Korf^{4,5}  | Charlotte von Gall¹

¹Institute of Anatomy II, Medical Faculty, Heinrich-Heine-University, Düsseldorf, Germany

²Zoology Department, Faculty of Science, Suez University, Suez, Egypt

³Department of Medicine 1, University Hospital Frankfurt, Frankfurt, Germany

⁴Institute of Anatomy I, Medical Faculty, Heinrich-Heine-University, Düsseldorf, Germany

⁵Institute of Anatomy II, Goethe University, Frankfurt, Germany

Correspondence

Horst-Werner Korf, Institute of Anatomy I, Medical Faculty, Heinrich-Heine-University, Universitätsstr. 1, 40225 Düsseldorf, Germany.

Email: korf@uni-duesseldorf.de

Abstract

Hepatocellular carcinoma (HCC) is highly resistant to anticancer therapy and novel therapeutic strategies are needed. Chronotherapy may become a promising approach because it may improve the efficacy of antimetabolic radiation and chemotherapy by considering timing of treatment. To date little is known about time-of-day dependent changes of proliferation and DNA damage in HCC. Using transgenic c-myc/transforming growth factor (TGF α) mice as HCC animal model, we immunohistochemically demonstrated Ki67 as marker for proliferation and γ -H2AX as marker for DNA damage in HCC and surrounding healthy liver (HL). Core clock genes (*Per1*, *Per2*, *Cry1*, *Cry2*, *Bmal 1*, *Rev-erba* and *Clock*) were examined by qPCR. Data were obtained from samples collected ex vivo at four different time points and from organotypic slice cultures (OSC). Significant differences were found between HCC and HL. In HCC, the number of Ki67 immunoreactive cells showed two peaks (ex vivo: ZT06 middle of day and ZT18 middle of night; OSC: CT04 and CT16). In ex vivo samples, the number of γ -H2AX positive cells in HCC peaked at ZT18 (middle of the night), while in OSC their number remained high during subjective day and night. In both HCC and HL, clock gene expression showed a time-of-day dependent expression ex vivo but no changes in OSC. The expression of *Per2* and *Cry1* was significantly lower in HCC than in HL. Our data support the concept of chronotherapy of HCC. OSC may become useful to test novel cancer therapies.

KEYWORDS

clock genes, hepatocellular carcinoma, Ki67, transgenic c-myc/TGF α mice, γ -H2AX

1 | INTRODUCTION

Hepatocellular carcinoma (HCC) ranks fourth among cancer-related mortalities worldwide with a mortality rate of 8.2% (782 000 deaths)

Abbreviation: CT, circadian time; DNA-DSBs, DNA-double-strand breaks; HCC, hepatocellular carcinoma; LD, light-dark; HL, healthy liver; OSC, organotypic slice culture; ZT, Zeitgeber time.

and with high new incidence cases (about 841 080) in 2018.¹ The most common causes of HCC are related to alcohol abuse and chronic infection with hepatitis B and C viruses which are accompanied with inflamed and cirrhotic liver. Some other risk factors include non-alcoholic fatty liver disease and hepatic manifestation of the metabolic syndrome due to obesity or diabetes.^{2,3} HCC, mostly diagnosed in advanced stages, is highly resistant to antimetabolic therapy. Several substances have been applied in the HCC patients including sorafenib

This is an open access article under the terms of the Creative Commons Attribution License, which permits use, distribution and reproduction in any medium, provided the original work is properly cited.

© 2020 The Authors. *International Journal of Cancer* published by John Wiley & Sons Ltd on behalf of Union for International Cancer Control.

and tivantinib. Sorafenib was also applied in combination with radiation (RT-SOR).^{4,5} However, these therapies have substantial side effects. The limited success of these therapies may in part be due to therapy in a phase in which the tumors are not particularly susceptible and determination of the optimal time point for therapies (chronotherapy) may improve their efficacy.⁶ Ki67 and γ -H2AX are good markers to predict the response of HCC therapies. Ki67 is one of the most important cell proliferation markers which is increased during the tumor development. It is expressed in the S phase and G2/M phases of the cell cycle. Its expression changes during the day and is regulated by the circadian clock.⁷⁻⁹ Because Ki67 is expressed only in proliferating cells, it is one of the most widely used proliferation markers in cancer cells.^{10,11} γ -H2AX is a marker for DNA damage and repair. Upon DNA damage, DNA double-strand breaks (DSBs) are formed which are characteristic for cancer cells due to mutated and unchecked cell cycles. DNA-DSBs are always followed by the phosphorylation of H2AX histone and the formation of a new phosphorylated protein called γ -H2AX which starts the DNA repair process. After DNA is repaired, γ -H2AX is dephosphorylated.^{12,13} γ -H2AX can be used as a marker of radio-sensitivity of cancer and the normal surrounding tissues, their ability to recover from damage and the efficacy of the cellular repair process. This helps to control the dosage, the effectiveness and frequency of radiation therapy in localized target.¹²

To evaluate any beneficial effect of chronotherapy, it is necessary to clarify whether cell proliferation and DNA repair mechanisms in HCC cells follow a diurnal pattern and whether this pattern differs from that in healthy liver (HL) tissue. These questions are addressed in the present study in an animal model for HCC, double transgenic *c-myc/TGF α* mice¹⁴ by immunohistochemical demonstration of Ki67 and γ -H2AX.

Cell cycle and proliferation are closely intertwined with the molecular circadian clockwork and there is increasing evidence that cancer development and progression may be associated with dysfunction or mutation of this molecular clockwork. We have therefore investigated whether the circadian molecular clockwork is altered in HCC as compared to healthy liver tissue. The molecular circadian clockwork comprises clock genes which interact in positive and negative transcription-translation feedback loops.^{15,16} Briefly, the expression of *Per* (*Per1* and *Per2*) and *Cry* (*Cry1* and *Cry2*) genes is activated by heterodimers of the transcription factors CLOCK/BMAL1 which act as the positive elements in the loop while dimers of PER/CRY form the negative loop.¹⁶ The molecular circadian clockwork ticks in all nucleated cells and governs many physiological processes by controlling the expression of more than 3000, so-called clock-controlled genes.

Finally, we have addressed the question whether results obtained by ex vivo samples are compared to those obtained by in vitro samples such as organotypic slice cultures (OSC) to evaluate whether OSC of liver and HCC represent adequate models to test novel anti-cancer therapies. Previous studies have shown that OSC which maintain the three-dimensional structure of the tissue and a functional extracellular matrix maintain the circadian rhythms for several days.¹⁷ Usage of OSC would allow much faster and more effective screening of any novel therapeutic strategy than experiments with whole animals.

What's new?

The acquisition of therapeutic resistance in hepatocellular carcinoma (HCC) is a major obstacle in chemotherapy-based approaches to HCC treatment. Therapeutic resistance may be attributed in part to the phase of tumor development at the time of therapy. Here, assessment of timing of antimetabolic therapies in an HCC animal model reveals time-of-day dependent changes in tumor cell proliferation and DNA damage. In addition, clock gene expression was altered in HCC, suggesting a link to tumor development and growth. The results indicate that the efficacy of antimetabolic therapies depends on proper timing and that this time dependency should be evaluated further.

2 | MATERIALS AND METHODS

2.1 | Experimental animals

The experiments described in our study were conducted according to accepted standards of humane animal care and were consistent with federal guidelines and Directive 2010/63/EU of the European Union. They were approved by the Regierungspräsidium Darmstadt (Gen. Nr. FU 1067). All experiments were performed with male *c-myc/TGF α* bitransgenic mice. The animals were generated by crossing homozygous metallothionein/TGF α and albumin/*c-myc* single transgenic mice in CD13B6CBA background in which hepatocarcinogenesis can be accelerated by zinc in the drinking water.

Food and water containing ZnCl₂ were supplied *ad libitum*. All animals were kept under normal light-dark (LD) cycle (12:12). The development and growth of HCCs was controlled by MRI as described recently.¹⁸

2.2 | Ex vivo investigations

Twelve animals were used for immunohistochemical and 12 animals for real-time PCR analyses. All animals investigated had either single or multiple tumors (Table 1). The animals were sacrificed at 4 different *Zeitgeber* time points: ZT00 (light on), ZT06, ZT12 (light off) and ZT18. For immunohistochemical investigations, the animals (n = 3/ZT) were anesthetized by a mixture of ketamine (100 mg/kg body weight, Rotexmedica, Trittau, Germany) and xylazine (10 mg/kg body weight, Rompun 2%, Bayer Leverkusen, Germany) through intraperitoneal injection and then perfused transcardially with 0.9% sodium chloride solution for 1 minute followed by approximately 100 mL 4% paraformaldehyde (PFA) in 0.1 M phosphate-buffered saline (PBS, pH 7.4) for 15 minutes. Perfusion during the night was performed under dim red light. Healthy liver tissues and tumors were excised and post-fixed separately in 4% PFA in PBS for 2 hours, cryoprotected with gradually increasing concentrations of sucrose (10%, 20% and 30%) and cryosectioned separately into 12 μ m thick serial sections. For qPCR

TABLE 1 Number, size and volume of tumors in each mouse investigated ex vivo for qPCR, immunocytochemistry or in slice preparations (OSC)

qPCR Mouse				
Mouse ID	Number of tumors	Size diameters (cm)	Tumor volume (cm ³)	Time point
500254/	1	0.85 × 1.03	0.3721	ZT00
500255R	1	1.0 × 0.76	0.2888	ZT00
500232/	6	0.65 × 0.99; 1.07 × 0.69; 0.16 × 0.19; 0.32 × 0.31; 0.27 × 0.21; 0.37 × 0.38	0.5136	ZT00
500204RR	2	1.19 × 0.89; 1.09 × 0.69	0.7308	ZT06
500200/	4	0.63 × 0.65; 0.62 × 0.66; 0.81 × 0.94; 1.32 × 1.65	2.002	ZT06
500210/	5	0.98 × 0.77; 0.51 × 0.63; 0.28 × 0.31; 0.26 × 0.3; 0.45 × 0.49	0.4444	ZT06
500228L	3	1.68 × 1.11; 0.31 × 0.38; 0.61 × 0.5	1.1295	ZT12
500242/	2	0.64 × 1.26; 0.27 × 0.42	0.2734	ZT12
500253L	2	1.16 × 1.26; 0.91 × 0.95	1.2411	ZT12
500230R	3	0.43 × 0.32; 0.73 × 1.12	0.3204	ZT18
500229/	3	0.35 × 0.49; 0.36 × 0.29; 0.2 × 0.17	0.0480	ZT18
500209RR	10	0.4 × 0.74; 0.66 × 0.48; 0.34 × 0.41; 0.4 × 0.43; 0.38 × 0.42; 0.58 × 0.5; 0.39 × 0.44; 0.97 × 0.74; 1.36 × 0.8; 0.66 × 0.74	1.193	ZT18
Immunostaining				
Mouse ID	Number of tumors	Size diameters (cm)	Tumor volume (cm ³)	Time point
463663L	1	1.2 × 0.61	0.2233	ZT00
463665RR	3	0.25 × 0.36; 0.22 × 0.26; 0.23 × 0.27	0.0247	ZT00
466832RL	2	0.2 × 0.32; 0.32 × 0.51	0.0325	ZT00
463664RL	1	1.34 × 0.68	0.3098	ZT06
466835R	4	0.70 × 0.69; 0.29 × 0.35; 0.32 × 0.37; 0.32 × 0.44	0.2228	ZT06
469617L	2	0.36 × 0.36; 0.24 × 0.21	0.0286	ZT06
463666LL	1	1.13 × 0.58	0.1901	ZT12
466836L	5	0.56 × 0.87; 0.64 × 0.44; 0.18 × 0.3; 0.27 × 0.23; 0.18 × 0.19	0.2134	ZT12
470729R	1	0.49 × 0.4	0.0392	ZT12
463662R	1	0.35 × 0.3	0.0158	ZT18
463667/	3	0.36 × 0.21; 0.45 × 0.3; 0.2 × 0.26	0.0334	ZT18
469615/	2	0.46 × 0.76; 1.37 × 1.5	1.6217	ZT18
OSC				
Mouse ID	Number of tumors	Size diameters (cm)	Tumor volume (cm ³)	
500166/	5	0.28 × 0.29; 0.34 × 0.29; 0.56 × 0.53; 0.87 × 0.83; 0.21 × 0.2	0.4082	
500146L	2	0.79 × 0.97; 0.44 × 0.51	0.3427	
500150R	4	0.75 × 0.44; 0.46 × 0.46; 0.55 × 0.39; 0.37 × 0.46	0.1946	
500158/	2	1.26 × 1.14; 0.81 × 0.8	1.0779	
500174L	2	0.94 × 0.7; 0.53 × 0.41	0.2748	
500176/	2	0.38 × 0.34; 0.87 × 0.61	0.1838	
500155R	1	0.86 × 0.67	0.1930	

Note: Time point indicates killing of the animals.

investigations, the animals (n = 3/ZT) were decapitated at ZT00 (light on), ZT06, ZT12 (light off) and ZT18 and healthy liver tissue and tumors were excised separately, frozen rapidly in liquid nitrogen and stored at -80°C until further use. The experiments during the night were performed under dim red light.

2.3 | In vitro investigations of organotypic slice cultures

For in vitro investigations, six animals were sacrificed at 10:00 AM (ZT04) and healthy liver tissue and tumors were freshly excised under

sterilized conditions and kept in cold storage solution (MACS tissue storage solution, Miltenyi Biotec, Bergisch Gladbach, Germany). Organotypic slice cultures (OSC) were prepared using a Krumdieck tissue chopper (TSE Systems, Bad Homburg, Germany). Healthy liver tissue and tumors were sliced separately in ice-cold sterilized Dulbecco's phosphate-buffered saline (DPBS) (Gibco by Life Technologies, Paisley, UK). The slices (250 μm thick) were transferred to cell culture inserts (0.4 μm pores, Falcon, Durham, North Carolina) which were put in six-well plates filled with 1 mL prewarmed culture medium modified after.¹⁹ The medium consisted of DMEM, supplemented with 10% fetal bovine serum, 100 U/mL penicillin, 0.1 mg/mL streptomycin, 10 mmol/L HEPES, 1 mg/mL insulin, 8 mg/mL ascorbic acid and 20 mmol/L sodium pyruvate. All slices were cultured under constant conditions of 37°C and 5% CO₂ for 24 hours. The slices from healthy liver tissue and tumors were harvested at four different circadian time (CT) points; CT04, CT10, CT16 and CT22. CT00 is defined as the onset of the former light phase (6:00 AM). Slices to be used for immunohistochemistry were fixed in 4% PFA in PBS for 12 hours. The fixed slices were cryoprotected with gradually increasing concentrations of sucrose (15 and 30%) for at least 24 hours and then cryosectioned separately into 10 μm thick serial sections. The unfixed slices were quickly frozen on liquid nitrogen and stored at -80°C for qPCR investigations.

2.4 | Immunofluorescence staining

Cell proliferation (Ki67) and DNA-DSBs (γ -H2AX) were investigated in *ex vivo* and OSC samples of healthy liver and tumors of *c-myc/TGF α* mice harvested at different ZTs and CTs. To reduce non-specific staining, sections were preincubated in normal goat serum (1:20) diluted in PBS with 0.3% Triton (PBST) for 1 hour at room temperature. Sections were then incubated with primary antibodies against Ki67 (1:200, KI6891C01, DCS, Hamburg, Germany) or against γ -H2A.X (1:100, #2577, Cell Signaling Technology, Frankfurt am Main, Germany) diluted in 1% bovine serum albumin (BSA) in PBST at room temperature overnight. On the next day, sections were incubated with the secondary goat antirabbit antibodies diluted in PBST (1:250, Alexa 568 for Ki67 or Alexa 488 for γ -H2AX, Life Technologies, San Diego, California) for 1 hour in darkness at room temperature. Finally, all sections were stained with Hoechst nucleus dye diluted in PBS (1:10 000) for 5 minutes in darkness at room temperature. The stained sections were covered by fluorescent mounting media (Dako, Glostrup, Denmark). To verify the results from the immunostaining, negative controls were incubated with the secondary antibodies only.

2.5 | Data acquisition

For the quantitative analysis of the number of cells which are positively stained with Ki67 or γ -H2AX, six representative images from each animal and each time point were taken using a confocal laser

microscope (Olympus Fluoview SC20, Japan) at 20 \times objective. For each type of staining, the microscope settings were kept constant. The number of positive cells was counted manually in a total area = 409.6 mm² using Photoshop CS3 program (v10, Adobe, San Jose, California) by an investigator not familiar with the experimental protocol.

2.6 | Real-time PCR

Total RNA from healthy liver and tumor tissue was extracted using RNeasy Plus Universal Mini Kit (QIAGEN, Hilden, Germany). RNA purity and concentration were measured using a Nano-Drop spectrophotometer. Then cDNA was synthesized from total RNA (1 μg) using Revert Aid First Strand cDNA Synthesis Kit (Thermo Scientific, Vilnius, Lithuania). Relative expression of mRNA for target genes was measured using quantitative real-time PCR (qRT-PCR; Step One Plus; Applied Biosystems), SYBR GREEN (Kapa Abi-Prism) and specific primers for clock genes (all Sigma Aldrich, Table 2). All PCR amplicates were examined by conventional PCR and gel analyses. Expression of target genes was normalized to β -actin. Relative mRNA expression of genes was finally calculated by use of the Pfaffl method.²⁰

2.7 | Statistical analysis

Statistics were calculated by using Graph Pad Prism 8 software. The results were expressed as mean \pm SE of the mean (SEM). The significant differences for circadian effect in healthy liver and tumor were tested by RM One-Way analysis of variance (ANOVA) for OSC

TABLE 2 qPCR list of primers

Gene	Sequence
mPer2 F	5'-CCAAACTGCTTGTCCAGGC-3'
mPer2 R	5'-ACCGCCTGTAGGATCTTCT-3'
mCry1 F	5'-CTT CTG TCT GAT GAC CAT GAT GA-3'
mCry1 R	5'-CCC AGG CCT TTC TTT CCA A-3'
mCry2 F	5'-AGG GCT GCC AAG TGC ATC AT-3'
mCry2 R	5'-AGG AAG GGA CAG ATG CCA ATA G-3'
mClock F	5'-CAC CGA CAA AGA TCC CTA CTG AT-3'
mClock R	5'-TGA GAC ATC GCT GGC TGT GT-3'
mPer1 F	5'-TGG CTC AAG TGG CAA TGA GTC-3'
mPer1 R	5'-GGC TCG AGC TGA CTG TTC ACT-3'
β -Actin F	5'-GGCTGTATCCCCTCCATGC-3'
β -Actin R	5'-CCAGTTGGTAAACAATGCCATGT-3'
Rev-erb α F	5'-GGT GCG CTT TGC ATC GTT-3'
Rev-erb α R	5'-GGT TGT GCG GCT CAG GAA-3'
Bmal F	5'-GTA GAT CAG AGG GCG ACA GC-3'
Bmal R	5'-CCT GTG ACA TTC TGC GAG GT-3'

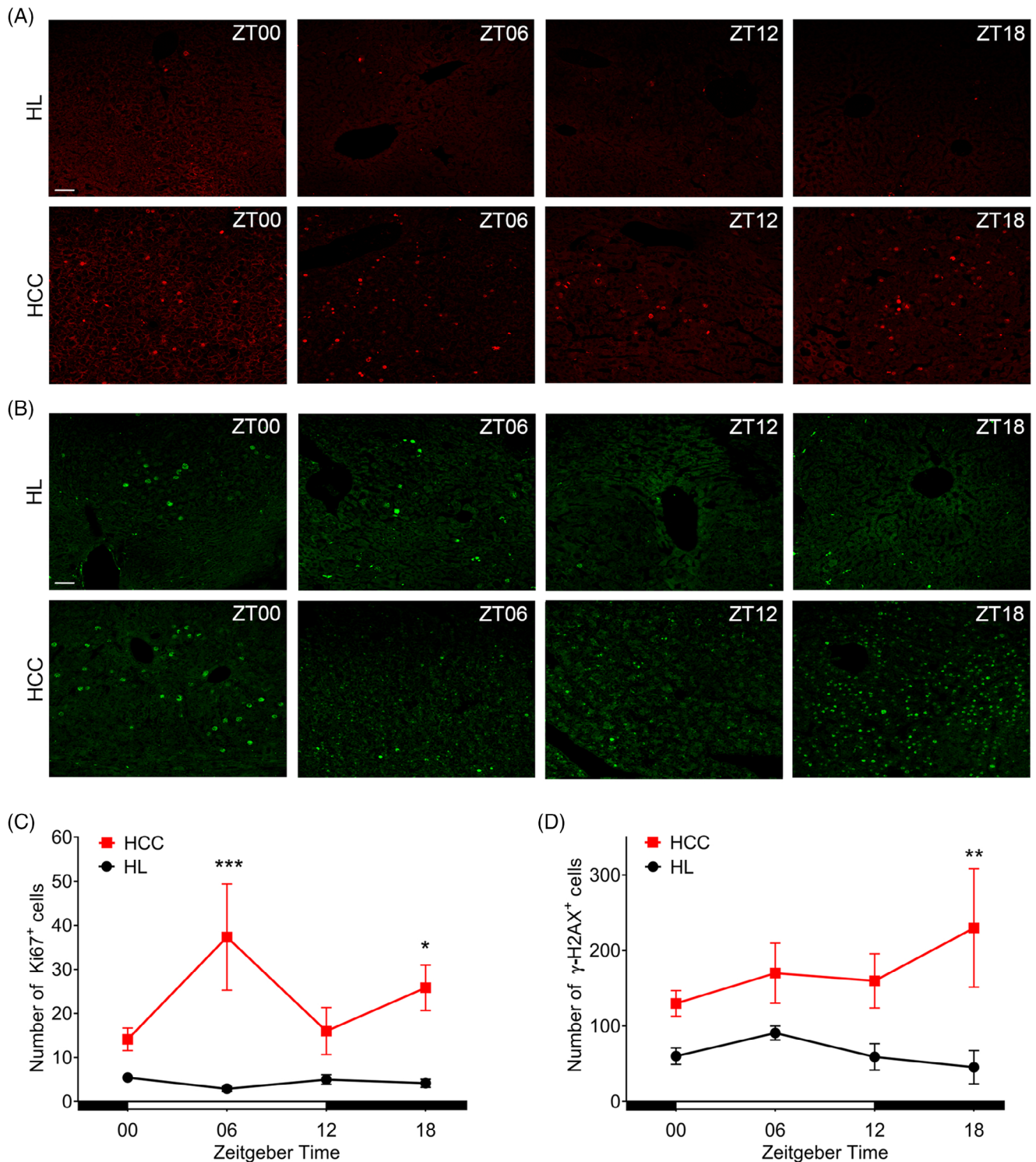


FIGURE 1 Ex vivo analyses of Ki67 and γ -H2AX in hepatocellular carcinoma (HCC) and surrounding healthy liver (HL) of *c-myc/TGF α* mice. The mice ($n = 3$ mice per time point) were killed at different *Zeitgeber* time (ZT) points, ZT00, ZT06, ZT12 and ZT18. A, Representative photomicrographs of Ki67 immunoreaction in HCC and HL at different ZTs. B, Representative γ -H2AX immunoreaction in HCC and HL at different ZTs. C, Number of Ki67 immunoreactive cells in HCC (red) and HL (black). D, Number of γ -H2AX immunoreactive cells in HCC (red) and HL (black). Plotted are the mean numbers \pm SEM of immunoreactive cells. White and black bars indicate day and night, respectively. * $P < .05$, ** $P < .01$, *** $P < .001$ differences between HCC and HL. Scale bars, 50 μ m [Color figure can be viewed at wileyonlinelibrary.com]

samples and Ordinary One-Way analysis of variance (ANOVA) for ex vivo samples followed by Tukey's test for multiple comparisons between different time points. Two-Way analysis of variance

(ANOVA) was used to validate differences according to time and tissue followed by Sidak's test for multiple comparisons between groups. The results were regarded as significant at $P < .05$.

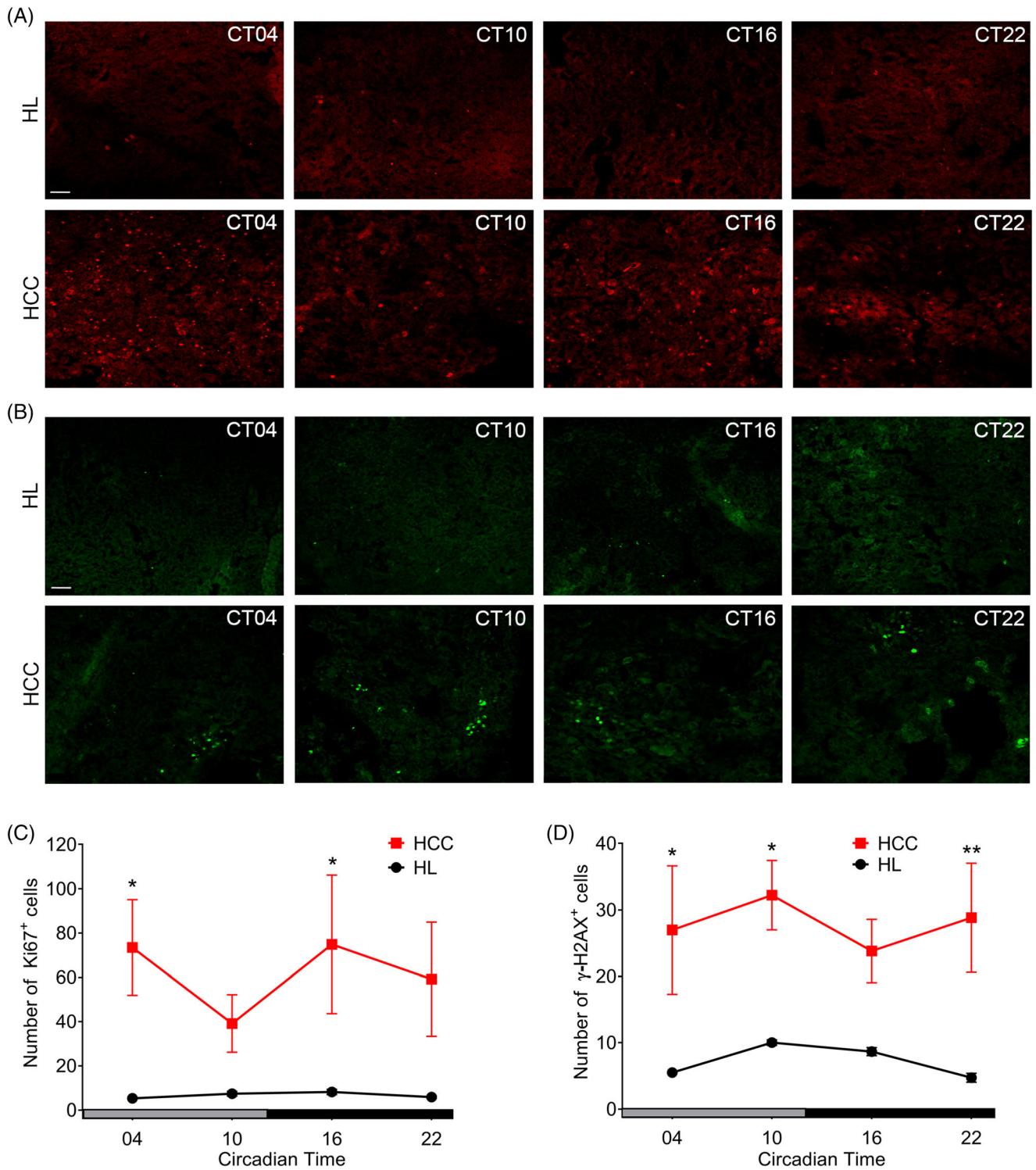


FIGURE 2 In vitro analyses of Ki67 and γ -H2AX in hepatocellular carcinoma (HCC) and the surrounding healthy liver (HL) of OSC from c-myc/TGF α mice. The slices (*n* = 6 per time point) were collected at different circadian time (CT) points. A, Representative photomicrographs of Ki67 immunoreaction in HCC and HL at different CTs. B, Representative γ -H2AX immunoreaction in HCC and HL at different CTs. C, Number of Ki67 immunoreactive cells in HCC (red) and HL (black). D, Number of γ -H2AX immunoreactive cells in HCC (red) and HL (black). Plotted are the mean numbers \pm SEM of immunoreactive cells. Gray and black bars indicate the former day and night, respectively. **P* < .05, ***P* < .01 differences between HCC and HL. Scale bars, 50 μ m [Color figure can be viewed at wileyonlinelibrary.com]

3 | RESULTS

3.1 | Investigation of Ki67 and γ -H2AX immunoreactivity in HCC and surrounding HL

These investigations were performed in both, ex vivo samples and OSC. In ex vivo samples, the number of Ki67 immunoreactive cells was very low in healthy liver and did not change significantly

at the four time points investigated. As expected, the number of Ki67 immunoreactive cells was higher in HCC than in HL (Figure 1A). In HCC, the number of Ki67 immunoreactive cells showed a maximum at midday (ZT06) and second, smaller peak at midnight (ZT18) and a minimum in the morning (ZT00; Figure 1C). The differences in the number of proliferating Ki67 immunoreactive cells between HCC and HL were very highly significant at ZT06 ($P < .001$) and significant at ZT18 ($P < .05$) as shown by

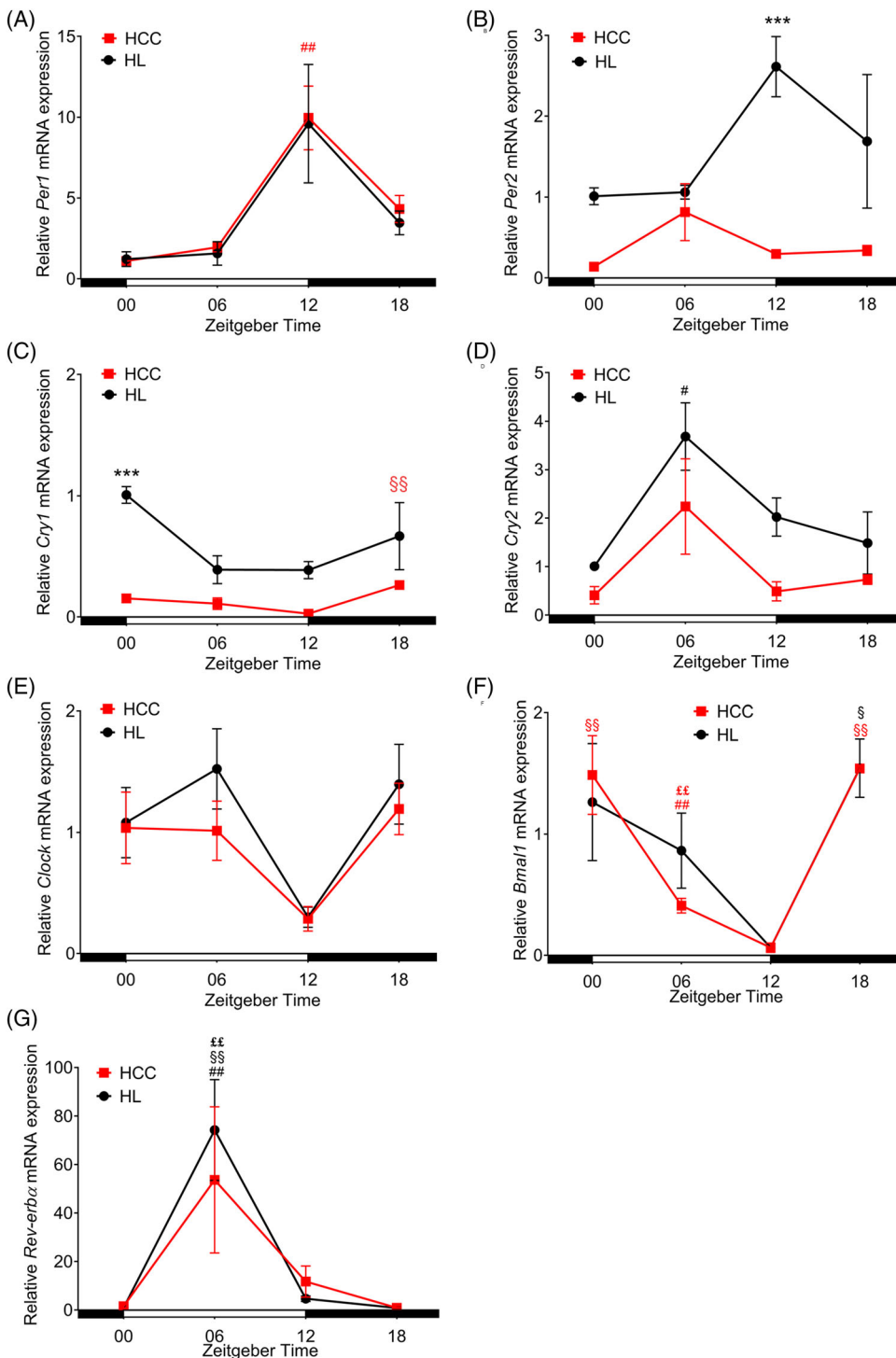


FIGURE 3 Ex vivo analyses of clock genes expression in hepatocellular carcinoma (HCC, red) and the surrounding healthy liver (HL, black) of c-myc/TGF α mice by real time qPCR. The mice (n = 3 mice per time point) were killed at different Zeitgeber time points. A, Relative expression of *Per1* in HCC and HL. B, Relative expression of *Per2* in HCC and HL. C, Relative expression of *Cry1* in HCC and HL. D, Relative expression of *Cry2* in HCC and HL. E, Relative expression of *Clock* in HCC and HL. F, Relative expression of *Bmal1* in HCC and HL. G, Relative expression of *Rev-erb α* in HCC and HL. Plotted are the mean relative mRNA expression \pm SEM of clock genes. White and black bars indicate day and night, respectively. *** $P < .001$ differences between HCC and HL. # $P < .05$; ## $P < .01$ differences between this ZT and ZT00. § $P < .05$; §§ $P < .01$ differences between this ZT and ZT12. ££ $P < .01$ differences between this ZT and ZT18 [Color figure can be viewed at wileyonlinelibrary.com]

two-way ANOVA followed by Sidak's multiple comparisons test (Figure 1C).

As a marker for DNA-DSBs repair, γ -H2AX immunoreactivity was investigated in the same ex vivo samples. The number of γ -H2AX immunoreactive cells was higher in HCC than in HL (Figure 1B). In HCC, the number of γ -H2AX immunoreactive cells showed a peak at midnight (ZT18). At ZT18, the difference between HCC and HL was highly significant ($P < .01$, Figure 1D).

Ki67 and γ -H2AX immunoreactivities were also investigated in OSC of HL and HCC of c-myc/TGF α mice. The OSC were cultured for 24 hours and thereafter fixed at four time points (CT04, CT10, CT16 and CT22). The number of Ki67 immunoreactive cells was higher in HCC than in HL (Figure 2A). Two-way ANOVA showed that the difference between HCC and HL was significant at CT04 and CT16 ($P < .05$, Figure 2C). The number of γ -H2AX immunoreactive cells was higher in HCC than in the surrounding HL. The differences in the number of γ -H2AX immunoreactive cells between HL and HCC were

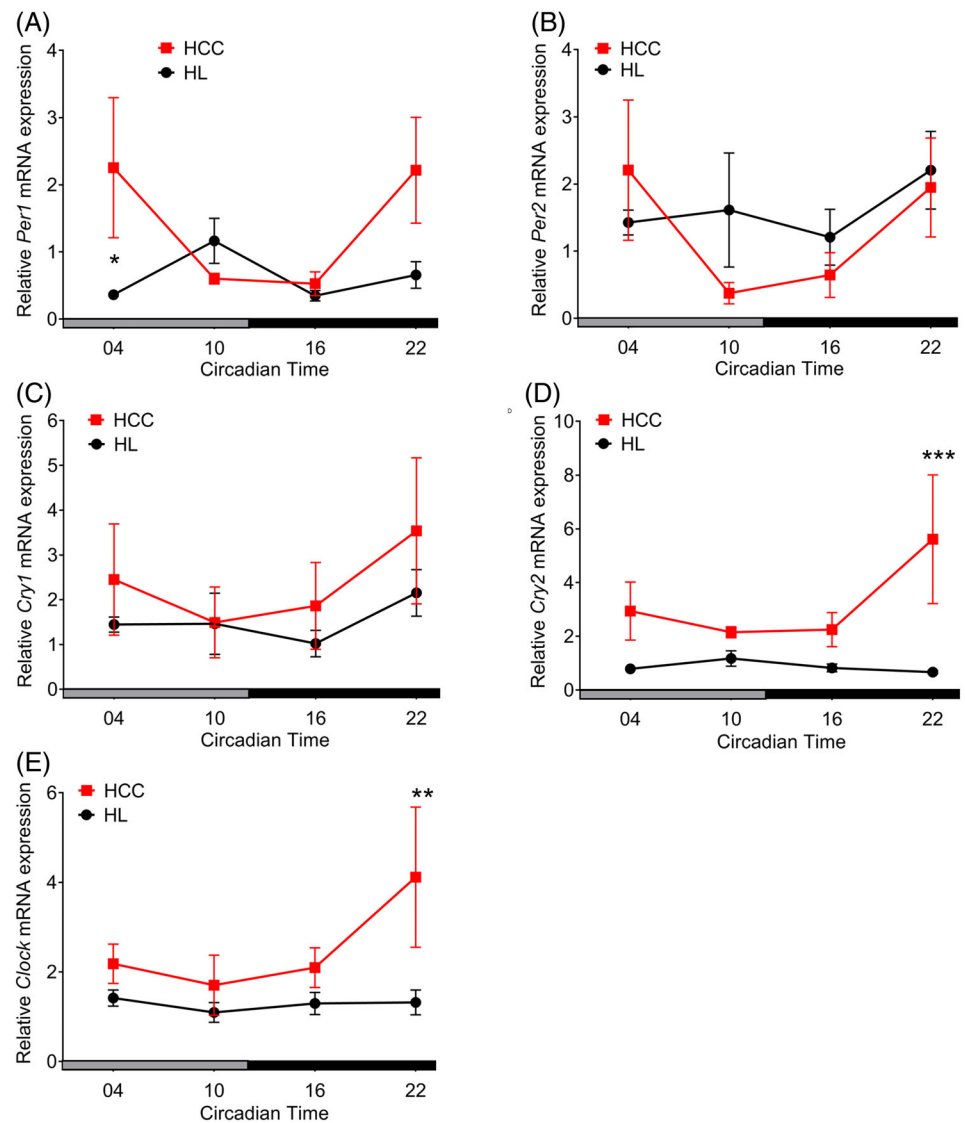
significant at CT04 and CT10 ($P < .05$) and highly significant at CT22 ($P < .01$; Figure 2D).

3.2 | Investigations of Clock genes expression in HCC and surrounding HL

Expression of clock genes *Per1*, *Per2*, *Cry1*, *Cry2* and *Clock* was investigated in HCC and HL using qPCR in both, ex vivo samples and OSC. In addition, expression of *Bmal 1* and *Rev-erb α* was analyzed in the ex vivo samples.

In ex vivo samples, the relative expression of *Per1* showed a peak at ZT12 in HL which tended to be different from ZT00 ($P = .058$) and ZT06 ($P = .07$). A peak at ZT12 was also observed in HCC which was significantly different from the values at ZT00 and ZT06 ($P < .01$) and at ZT18 ($P < .05$; Figure 3A). The relative expression of *Per1* did not differ significantly between HL and HCC at all time points investigated ($P > .1$, Figure 3A).

FIGURE 4 In vitro analyses of clock genes expression in hepatocellular carcinoma (HCC, red) and the surrounding healthy liver (HL, black) of OSC from c-myc/TGF α mice. The slices ($n = 6$ per time point) were collected at different circadian time points. A, Relative expression of *Per1* in HCC and HL. B, Relative expression of *Per2* in HCC and HL. C, Relative expression of *Cry1* in HCC and HL. D, Relative expression of *Cry2* in HCC and HL. E, Relative expression of *Clock* in HCC and HL. Plotted are the mean relative mRNA expression \pm SEM of clock genes. Gray and black bars indicate the former day and night, respectively. * $P < .05$, ** $P < .01$ and *** $P < .001$ differences between HCC and HL [Color figure can be viewed at wileyonlinelibrary.com]



The relative expression of *Per2* in HL did not change significantly between day and night (Figure 3B). The relative expression of *Per2* was decreased in HCC as compared to the surrounding HL and this difference was highly significant at ZT12 ($P < .001$, Figure 3B).

The relative expression of *Cry1* in HL showed a maximum at ZT00 which tended to be different from the values at ZT06 and ZT12 ($P = .09$). In contrast, the HCC showed a peak at ZT18 which was significantly different from the values at ZT12 ($P < .01$) and ZT06 ($P < .05$; Figure 3C). The relative expression of *Cry1* was lower in HCC than in HL and the two-way ANOVA showed that this difference was significantly different at ZT00 ($P < .001$) and tended to be significant at ZT18 ($P = .09$, Figure 3C).

The relative expression of *Cry2* in HL showed a peak at (ZT06) which was significantly different from the values at ZT00 ($P < .05$) and tended to be different from those at ZT18 ($P = .06$). The relative expression of *Cry2* in HCC showed no significant changes during the day ($P > .1$, Figure 3D). The relative expression of *Cry2* was lower in HCC than the HL although the difference between HCC and HL was not significant at all investigated time points as shown by two-way ANOVA ($P > .1$, Figure 3D).

The relative expression of *Clock* changed during the day in the HCC and the surrounding HL. The values at ZT12 tended to be different from those at ZT06 ($P = .056$) and ZT18 ($P = .09$) in the HL and at ZT18 ($P = .08$) (Figure 3E) in the HCC. No significant changes were detected comparing the relative expression of *Clock* in HL and the HCC at the all investigated time points using the two-way ANOVA test ($P > .1$, Figure 3E).

The relative expression of *Bmal 1* in HL and HCC revealed a peak at (ZT18) which significantly differed from the values at ZT12 ($P < .05$ and $P < .01$; respectively). In HCC, ZT18 also showed a significant difference from ZT06 ($P < .01$). The value at ZT00 was significantly different from ZT06 and ZT12 ($P < .01$, Figure 3F). The relative expression of *Bmal* did not differ significantly between HL and HCC at all time points investigated ($P > .1$, Figure 3F).

The relative expression of *Rev-erb α* in HL showed a maximum at ZT06 which was significantly different from the values at ZT00, ZT12 and ZT18 ($P < .01$, Figure 3G). A maximum at ZT06 was also observed in HCC but it did not differ significantly from the other ZTs. No significant differences were detected comparing the relative expression of *Rev-erb α* in HL and HCC at all time points investigated. In the OSC, the relative expression of *Per1*, *Per2*, *Cry1*, *Cry2* and *Clock* showed a trend to daily variation in HCC and HL but the differences were not significant between day and night ($P > .1$, Figure 4). The relative expression was significantly higher in HCC than in HL for *Per1* at CT04 ($P < .05$), for *Cry2* at CT22 ($P < .001$) and for *Clock* at CT22 ($P < .01$; Figure 4, two-way ANOVA followed by Sidak's multiple comparisons test).

4 | DISCUSSION

An important topic in oncology is whether timing plays a role in anti-mitotic therapy. Taking this topic into consideration we have

addressed three questions in the present study: (a) Do cell proliferation and DNA damage repair mechanisms show a distinct temporal pattern that would help to determine the optimal time point(s) for antimetabolic therapy? (b) Does the expression of clock genes differ between normal and tumor tissue? (c) Are organotypic slice cultures an appropriate model to determine the optimal time point(s) for antimetabolic therapies? The investigations were performed with a well-established animal model for hepatocellular carcinomas, the double transgenic *c-myc/TGF α* mice.

4.1 | Do cell proliferation and DNA damage repair mechanisms show a distinct temporal pattern that would help to determine the optimal time point(s) for antimetabolic therapy?

Markers which reflect cell proliferation and DNA damage repair mechanisms are used for early detection of tumors, prediction of tumor development and assessment of the tumor response to therapy.¹³ We have assessed cell proliferation by means of immunohistochemical demonstration of Ki67, a nuclear antigen expressed in proliferating cells. As biomarker for DNA damage and repair,^{10,13} we have investigated γ -H2AX.

Our investigations of ex vivo samples revealed that the number of Ki67 immunoreactive cells was much higher in the HCC than in the surrounding HL. Lin et al²¹ reported that Wee1 (one of the cell cycle mitotic inhibitor) was decreased, while Cyclin B and CDC2 (cell cycle control genes) and cell cycle-related proteins (eg, cyclin A) were over-expressed in the HCCs as compared to healthy, noncancerous liver tissue. This disturbance in the expression of cell cycle regulators could explain the higher number of proliferating rate (Ki67) in HCC as compared to the surrounding HL.²¹

In HCC, the number of Ki67 immunoreactive cells showed a maximum at midday (ZT06) and second, smaller peak at midnight (ZT18). These results are in agreement with a study by You et al²² who showed that mammary tumors had two daily growth rate peaks, one minor at mid-sleep and one major peak at mid-activity. Two proliferation peaks were also observed in other fast-growing tumors.^{9,23} In an early study, fast and slow growing hepatomas showed two mitotic activity peaks, one during the light phase and the other during dark phase.²⁴ It is well known that the expression of cell cycle regulators which either promote or inhibit cell proliferation are affected by the circadian clockwork. In mammary tumor, the expression of some known clock-controlled cell cycle genes which promote cell proliferation, such as *CycD1* and *C-Myc* as well as cancer cell mitosis showed two peaks during the day, one at mid-day and the other at the midnight,^{22,25} whereas only one peak was found in healthy tissue.

A highly relevant result of our ex vivo studies was that the difference in number of proliferating Ki67 immunoreactive cells between the HCC and the HL was significant at ZT06 (midday) and at ZT18 (midnight). Since it is well known that highly proliferating cells become more sensitive to DNA damage with cancer therapies,^{26,27} we conclude that midday and midnight may be considered as optimal time

points to apply antimetabolic therapies to HCC with minimum side effects on the surrounding HL. This assumption now needs to be confirmed in further experiments. Since the two peaks occurred at mid-day and midnight, the findings in nocturnal species (mouse) might be easily transferred to diurnal species (eg, primates).

We then investigated γ -H2AX, a histone which accumulates in the damaged sites of DNA-DSBs in ex vivo samples. The number of γ -H2AX immunoreactive cells was higher in the HCC than in the surrounding HL. This conforms to previous investigations by Kim et al²⁸ and Matsuda et al²⁹ who showed that γ -H2AX was significantly increased in different human liver diseases including chronic hepatitis, HBV-related liver cirrhosis and HBV-related HCC as compared to normal and noncancerous tissues. Increased levels of γ -H2AX were also found in human tumors of the urinary bladder, breast, lung and colon.^{30,31}

As shown by our study the number of γ -H2AX immunoreactive cells showed a trend to daily variation in the HCC and the surrounding HL. The mechanism behinds these changes remain to be elucidated. One possibility is that ATM \rightarrow Chk2 signaling pathway which is mainly activated by double-strand breaks is subjected to the circadian rhythm of the clock genes.³² Other publications also reported that cellular responses to DNA damage and repair process are influenced by the circadian rhythm. XPA, one of the DNA repair protein, was shown to be controlled by the circadian clock in the mouse brain, liver and skin.³³⁻³⁵ Kang et al³⁴ found that the activity of nucleotide excision repair (NER) is highest in the afternoon/evening hours and lowest in the night/early morning hours in mouse brain. Thus, it is very important in cancer treatment protocols to take into consideration the circadian oscillation of cellular DNA repair molecules.

4.2 | Does the expression of clock genes differ between healthy and tumor tissue?

Cell cycle and proliferation are closely intertwined with the molecular circadian clockwork and there is increasing evidence that cancer development and progression may be associated with dysfunction or mutation of this molecular clockwork. We therefore investigated the expression of seven core clock genes, *Per1*, *Per2*, *Cry1*, *Cry2*, *Bmal 1*, *Rev-erba* and *Clock*, in HL and HCC at four different time points. Relative mRNA expression of all seven clock genes was shown to change between day and night in HL of c-myc/TGF α bitransgenic mice. Similar patterns were found in HL of non-transgenic mice.³⁶ Notably, mRNA expression of *Per1*, *Cry2*, *Bmal 1*, *Rev-erba* and *Clock* in the HCC had the same daily patterns as in the HL with similar peaks. In line with these results, Yang et al³⁷ reported that the daily expression of core clock genes maintains circadian rhythms within normal and tumor tissues of mice and concluded that the circadian clock remains functional in tumors. Two studies on buccal mucosal carcinogenesis showed that the daily rhythmic mRNA expression of *Per1* and *Per2* was similar in normal buccal mucosa and carcinoma stages and the acrophase occurred at approximately the same time.^{8,38}

Notably, in our study, the peaks of mRNA expression of *Per2* and *Cry1* differed between the HCC and the surrounding HL and the expression of *Per2*, *Cry1* and *Cry2* was lower in the HCC than the surrounding HL. Lowered expression of *Per2* and *Cry2* was also observed in human HCC^{21,39} and the amplitude of *Cry1* and *Cry2* were decreased in mouse livers treated with diethylnitrosamine and in human colorectal liver metastasis.^{40,41} Downregulation of different core clock genes was also reported in gastric, colorectal, pancreatic, prostate, breast, lung cancer, chronic lymphocytic leukemia, colorectal liver metastasis and HCC.³⁹⁻⁴²

Downregulation of clock genes may result from a hypoxic microenvironment which is a common feature in most solid tumors. Although HCC is one of the most hypervascularized types of tumors, it contains hypoxic regions due to rapid cell proliferation and the formation of aberrant blood vessels. Hypoxia can activate HIF-1 α and HIF-1 β and the overexpression of these transcription factors may contribute to the disturbed expression of clock genes in HCC cells. HIF also controls the expression of glycolytic enzymes which are responsible for acidic tumor environment, and this acidity is thought to act on the tumor cellular clocks.^{21,43,44} Downregulation of clock genes may also relate to the overexpression of factors that play an important role in the methylation of gene promoters which lead to inhibition of gene expressions as well as phosphorylation and degradation of clock genes. Thus, EZH2 and CK1 ϵ gene expression levels were strongly increased in HCC and colorectal liver metastasis, as compared to noncancerous tissues.^{21,42,43}

Our data showed no changes in the expression of the *Bmal 1*, *Rev-erba* and *Clock* gene in the HCC as compared to the surrounding HL. The same results were reported also for *Bmal1* and *Clock* in the human HCC.^{21,45} The reason for this is unclear and further studies are needed to clarify whether downregulation of some clock genes is associated with more advanced cancer stages.⁴⁶

The *Per2* gene appears to be a functionally more relevant in the mammalian circadian clock than the *Per1* gene.⁴⁷ Lower expression of *Per2* was shown to elicit more profound effects on the tumor growth, both in vitro and in vivo than lower expression of *Per1*.²⁵ In gastric cancer, the *Per2* expression was reported to be a potential prognostic factor and lower expression of *Per2* might help identify gastric cancer patients with a poor prognosis. Also, in chronic lymphocytic leukemia, the ratio between PER2 and CRY1 is suggested to be a prognostic marker that predicts the survival outcomes of patients.⁴³ In line with these results, *Per2* and *Cry1* may play a more important role for cell cycle disruption and HCC growth than the other core clock genes investigated here.

4.3 | Are organotypic slice cultures an appropriate model to determine the optimal time point(s) for anticancer therapies?

OSC is a model which is made from primary tissue and maintains the three-dimensional structure as well as the extracellular matrix.⁴⁸ OSC of normal liver was shown to be viable in culture conditions for several days and to keep a robust circadian rhythm.^{17,49} The present study with OSC which includes HCC and the surrounding HL showed

that the number of Ki67 and γ -H2AX immunoreactive cells was much higher in the HCC than in the HL as was also observed in ex vivo samples. The number of Ki67 immunoreactive cells showed two peaks which occurred at CT04 and CT16 and thus slightly differed from the time points which were observed in the ex vivo samples (ZT06 and ZT18). Notably, also the expression pattern and amplitudes of the clock genes differed between the OSC and ex vivo samples. This difference may be due to the lack of entrainment signals which under in vivo conditions are transmitted derived from the master oscillator of the circadian system, the suprachiasmatic nucleus, to the periphery via neuronal pathways or the blood stream. It is well known that temperature can act as physical synchronizer and resetting cue for circadian peripheral oscillators.⁵⁰ The fact that the temperature was kept constant in our culture experiments may contribute to the differences between OSC and ex vivo samples, although previous studies using identical, constant culture conditions^{17,49} have shown that OSC kept a robust circadian rhythm under constant temperature. The stress generated by the dissection process and the initiation of the culture may also contribute to these observed differences. The results suggest that OSC may be helpful to establish therapeutic strategies, but it remains to be established whether are suited to determine the optimal time points of antimetabolic therapies.

In conclusion, our study with an experimental mouse model for hepatocellular carcinoma showed significant differences in proliferation rate as well as DNA damage and repair mechanisms between the HCC and the HL. The observation that the proliferation rate in the HCC showed two distinct peaks indicates that the efficacy of antimetabolic therapies depends on the timing. Future studies in oncology should consider this time dependency and determine the optimal time point(s) for anticancer therapy for each tumor entity. Since γ -H2AX expression was higher in the HCC than in the HL, it can be used as a marker to determine HCC sensitivity to the antimetabolic treatment. Since expressions of *Per2* and *Cry1* were significantly lower and had different daily variation patterns in the HCC and the HL, these two clock genes might be closely linked to development and growth of the HCC. Overall, OSC may become a suitable model to develop and test anticancer strategies; however, future studies are needed to prove whether they could substitute for whole animal studies with regard to determination of the optimal time points for therapy.

ACKNOWLEDGEMENTS

S. A. H. is supported by German Egyptian Research Long-term Scholarship (GERLS) Program of the DAAD. We are grateful to Prof Nürnbergger (Institute of Anatomy II, Goethe University, Frankfurt am Main, Germany) for continuous support and advice. We thank Snorri Thorgeirsson (National Cancer Institute, NIH, Bethesda) for providing the mice transgenic for c-myc and TGF α . We thank Hanna Bellert, Ralf Fassbender, Angelika Hallenberger and Ursula Lammersen for excellent technical support. Open access funding enabled and organized by Projekt DEAL.

CONFLICT OF INTEREST

The authors have no conflict of interest.

DATA AVAILABILITY STATEMENT

The data will be made available upon reasonable request. https://www.researchgate.net/profile/Horst-Werner_Korf.

ETHICS STATEMENT

The experiments described in our study were conducted according to accepted standards of humane animal care and were consistent with federal guidelines and Directive 2010/63/EU of the European Union. They were approved by the Regierungspräsidium Darmstadt (Gen. Nr. FU 1067).

ORCID

Horst-Werner Korf  <https://orcid.org/0000-0002-5051-0303>

REFERENCES

1. IARC. Latest global cancer data: cancer burden rises to 18.1 million new cases and 9.6 million cancer deaths in 2018. No. 263. Press Release; 2018.
2. Trojan J, Zangos S, Schnitzbauer AA. Diagnostics and treatment of hepatocellular carcinoma in 2016: standards and developments. *Visc Med.* 2016;32:116-120.
3. Schlageter M, Terracciano LM, D'Angelo S, Sorrentino P. Histopathology of hepatocellular carcinoma. *World J Gastroenterol.* 2014;20:15955-15964.
4. Wild AT, Gandhi N, Chettiar ST, et al. Concurrent versus sequential sorafenib therapy in combination with radiation for hepatocellular carcinoma. *PLoS One.* 2013;8:e65726.
5. Rebouissou S, La Bella T, Reki S, et al. Proliferation markers are associated with MET expression in hepatocellular carcinoma and predict Tivantinib sensitivity in vitro. *Clin Cancer Res.* 2017;23:4364-4375.
6. Ballesta A, Innominato PF, Dallmann R, Rand DA, Levi FA. Systems Chronotherapeutics. *Pharmacol Rev.* 2017;69:161-199.
7. Liu SL, Han Y, Zhang Y, et al. Expression of metastasis-associated protein 2 (MTA2) might predict proliferation in non-small cell lung cancer. *Target Oncol.* 2012;7:135-143.
8. Ye H, Yang K, Tan XM, Fu XJ, Li HX. Daily rhythm variations of the clock gene PER1 and cancer-related genes during various stages of carcinogenesis in a golden hamster model of buccal mucosa carcinoma. *Onco Targets Ther.* 2015;8:1419-1426.
9. Wood PA, Du-Quito J, You S, Hrushesky WJ. Circadian clock coordinates cancer cell cycle progression, thymidylate synthase, and 5-fluorouracil therapeutic index. *Mol Cancer Ther.* 2006;5:2023-2033.
10. Shi W, Hu JF, Zhu SZ, et al. Expression of MTA2 and Ki-67 in hepatocellular carcinoma and their correlation with prognosis. *Int J Clin Exp Pathol.* 2015;8:13083-13089.
11. Sun X, Kaufman PD. Ki-67: more than a proliferation marker. *Chromosoma.* 2018;127:175-186.
12. Kuo LJ, Yang L. γ -H2AX—a novel biomarker for DNA double-strand breaks. *In Vivo.* 2008;22:305-310.
13. Sedelnikova OA, Bonner WM. GammaH2AX in cancer cells: a potential biomarker for cancer diagnostics, prediction and recurrence. *Cell Cycle.* 2006;5:2909-2913.
14. Thorgeirsson SS, Santoni-Rugiu E. Transgenic mouse models in carcinogenesis: interaction of c-myc with transforming growth factor alpha and hepatocyte growth factor in hepatocarcinogenesis. *Br J Clin Pharmacol.* 1996;42:43-52.
15. Schibler U, Ripperger J, Brown SA. Peripheral circadian oscillators in mammals: time and food. *J Biol Rhythms.* 2003;18:250-260.
16. Korf H-W, von Gall C. Circadian physiology. In: Pfaff DW, ed. *Neuroscience in the 21st Century: From Basic to Clinical.* New York, NY: Springer; 2013:1813-1845.

17. Muller MH, Rodel F, Rub U, Korf HW. Irradiation with X-rays phase-advances the molecular clockwork in liver, adrenal gland and pancreas. *Chronobiol Int.* 2015;32:27-36.
18. Schmithals C, Koberle V, Korkusuz H, et al. Improving drug penetrability with iRGD leverages the therapeutic response to Sorafenib and doxorubicin in hepatocellular carcinoma. *Cancer Res.* 2015;75:3147-3154.
19. Verrill C, Davies J, Millward-Sadler H, Sundstrom L, Sheron N. Organotypic liver culture in a fluid-air interface using slices of neonatal rat and adult human tissue—a model of fibrosis in vitro. *J Pharmacol Toxicol Methods.* 2002;48:103-110.
20. Pfaffl MW. Quantification strategies in real-time PCR. In: Bustin SA, ed. *A-Z of quantitative PCR.* La Jolla, CA: International University Line (IUL); 2004:87-112.
21. Lin YM, Chang JH, Yeh KT, et al. Disturbance of circadian gene expression in hepatocellular carcinoma. *Mol Carcinog.* 2008;47:925-933.
22. You S, Wood PA, Xiong Y, Kobayashi M, Du-Quiton J, Hrushesky WJ. Daily coordination of cancer growth and circadian clock gene expression. *Breast Cancer Res Treat.* 2005;91:47-60.
23. Kobayashi M, Wood PA, Hrushesky WJM. Circadian chemotherapy for gynecological and genitourinary cancers. *Chronobiol Int.* 2009;19:237-251.
24. Echave Llanos JM, Nash RE. Mitotic circadian rhythm in a fast-growing and a slow-growing hepatoma: mitotic rhythm in hepatomas. *J Natl Cancer Inst.* 1970;44:581-585.
25. Yang X, Wood PA, Ansell CM, et al. The circadian clock gene Per1 suppresses cancer cell proliferation and tumor growth at specific times of day. *Chronobiol Int.* 2009;26:1323-1339.
26. Shukla P, Gupta D, Bisht SS, et al. Circadian variation in radiation-induced intestinal mucositis in patients with cervical carcinoma. *Cancer.* 2010;116:2031-2035.
27. Rahn DA 3rd, Ray DK, Schlesinger DJ, et al. Gamma knife radiosurgery for brain metastasis of non-small cell lung cancer: is there a difference in outcome between morning and afternoon treatment? *Cancer.* 2011;117:414-420.
28. Kim H, Oh BK, Roncalli M, et al. Large liver cell change in hepatitis B virus-related liver cirrhosis. *Hepatology.* 2009;50:752-762.
29. Matsuda Y, Wakai T, Kubota M, et al. DNA damage sensor gamma-H2AX is increased in preneoplastic lesions of hepatocellular carcinoma. *ScientificWorldJournal.* 2013;2013:597095.
30. Bartkova J, Bakkenist CJ, Rajpert-De Meyts E, et al. ATM activation in normal human tissues and testicular cancer. *Cell Cycle.* 2005;4:838-845.
31. Gorgoulis VG, Vassiliou LV, Karakaidos P, et al. Activation of the DNA damage checkpoint and genomic instability in human precancerous lesions. *Nature.* 2005;434:907-913.
32. Sancar A, Lindsey-Boltz LA, Kang TH, Reardon JT, Lee JH, Ozturk N. Circadian clock control of the cellular response to DNA damage. *FEBS Lett.* 2010;584:2618-2625.
33. Corra S, Salvadori R, Bee L, Barbieri V, Mognato M. Analysis of DNA-damage response to ionizing radiation in serum-shock synchronized human fibroblasts. *Cell Biol Toxicol.* 2017;33:373-388.
34. Kang TH, Lindsey-Boltz LA, Reardon JT, Sancar A. Circadian control of XPA and excision repair of cisplatin-DNA damage by cryptochrome and HERC2 ubiquitin ligase. *Proc Natl Acad Sci U S A.* 2010;107:4890-4895.
35. Gaddameedhi S, Selby CP, Kaufmann WK, Smart RC, Sancar A. Control of skin cancer by the circadian rhythm. *Proc Natl Acad Sci U S A.* 2011;108:18790-18795.
36. Huisman SA, Oklejewicz M, Ahmadi AR, et al. Colorectal liver metastases with a disrupted circadian rhythm phase shift the peripheral clock in liver and kidney. *Int J Cancer.* 2015;136:1024-1032.
37. Yang X, Wood PA, Oh EY, Du-Quiton J, Ansell CM, Hrushesky WJ. Down regulation of circadian clock gene period 2 accelerates breast cancer growth by altering its daily growth rhythm. *Breast Cancer Res Treat.* 2009;117:423-431.
38. Tan XM, Ye H, Yang K, et al. Circadian variations of clock gene Per2 and cell cycle genes in different stages of carcinogenesis in golden hamster buccal mucosa. *Sci Rep.* 2015;5:9997.
39. Mteyrek A, Filipiński E, Guettier C, Okyar A, Levi F. Clock gene Per2 as a controller of liver carcinogenesis. *Oncotarget.* 2016;7:85832-85847.
40. Deng F, Yang K. Current status of research on the period family of clock genes in the occurrence and development of cancer. *J Cancer.* 2019;10:1117-1123.
41. Huisman SA, Ahmadi AR, JN IJ, Verhoef C, van der Horst GT, de Bruin RW. Disruption of clock gene expression in human colorectal liver metastases. *Tumour Biol.* 2016;37:13973-13981.
42. Oshima T, Takenoshita S, Akaike M, et al. Expression of circadian genes correlates with liver metastasis and outcomes in colorectal cancer. *Oncol Rep.* 2011;25:1439-1446.
43. Morgan M, Dvuchbabny S, Martinez C-A, Kerr B, Cistulli PA, Cook KM. The cancer clock is (not) ticking: links between circadian rhythms and cancer. *Clocks & Sleep.* 2019;1:435-458.
44. Yu C, Yang SL, Fang X, Jiang JX, Sun CY, Huang T. Hypoxia disrupts the expression levels of circadian rhythm genes in hepatocellular carcinoma. *Mol Med Rep.* 2015;11:4002-4008.
45. Yang SL, Yu C, Jiang JX, Liu LP, Fang X, Wu C. Hepatitis B virus X protein disrupts the balance of the expression of circadian rhythm genes in hepatocellular carcinoma. *Oncol Lett.* 2014;8:2715-2720.
46. Li HX. The role of circadian clock genes in tumors. *Onco Targets Ther.* 2019;12:3645-3660.
47. Zhao H, Zeng ZL, Yang J, et al. Prognostic relevance of Period1 (Per1) and Period2 (Per2) expression in human gastric cancer. *Int J Clin Exp Pathol.* 2014;7:619-630.
48. Palma E, Doornebal EJ, Chokshi S. Precision-cut liver slices: a versatile tool to advance liver research. *Hepatol Int.* 2019;13:51-57.
49. Yoo SH, Yamazaki S, Lowrey PL, et al. PERIOD2::LUCIFERASE real-time reporting of circadian dynamics reveals persistent circadian oscillations in mouse peripheral tissues. *Proc Natl Acad Sci USA.* 2004;101:5339-5346.
50. Buhr ED, Yoo SH, Takahashi JS. Temperature as a universal resetting cue for mammalian circadian oscillators. *Science.* 2010;330:379-385.

How to cite this article: Hassan SA, Schmithals C, von Harten M, Piiper A, Korf H-W, von Gall C. Time-dependent changes in proliferation, DNA damage and clock gene expression in hepatocellular carcinoma and healthy liver of a transgenic mouse model. *Int. J. Cancer.* 2021;148:226–237.
<https://doi.org/10.1002/ijc.33228>